Versatile CO_2 hydrogenation-dehydrogenation catalysis with Ru-PNP/ionic liquid system

Luca Piccirilli,[1] Brenda Rabell,[1] Rosa Padilla,[1] Anders Riisager,[1] Shoubhik Das,[2] Martin Nielsen[1]**

[1] *Department of Chemistry, Technical University of Denmark, DK-2800 Kgs. Lyngby, Denmark*

[2] *Department of Chemistry, Universiteit Antwerpen, Antwerp 2020, Belgium*

* *Correspondence: shoubhik.das@uantwerpen.be; Tel.: +32-653226*

* *Correspondence: marnie@kemi.dtu.dk; Tel.: +45-24651045*

ABSTRACT: High catalytic activities of Ru-PNP complexes in ionic liquid (IL) were obtained for the reversible hydrogenation of CO_2 and dehydrogenation of formic acid (FA) under exceedingly mild conditions. The novel catalytic system relies on an unprecedented IL-promoted activation of CO_2 and proceeds already at 25 ºC under a continuous flow of 1 bar of CO_2/H_2, leading to 14 mol% FA with respect to the IL, whereas a pressure of 40 bar of CO_2/H_2 (1:1) provides 126 mol% of FA/IL. The conversion of CO_2 contained in imitated biogas was also achieved at 25 ºC. Furthermore, the Ru-PNP/IL system catalyzes FA dehydrogenation with turnover frequencies (TOF) up to 11,000 h^{-1} under heat-integrated conditions for proton-exchange membrane (PEM) fuel cell applications (<100 ºC). Thus, 4 mL of a 0.005 M Ru-PNP/IL system converted 14.5 L FA over four months with a turnover number (TON) exceeding 18,000,000. Finally, 13 hydrogenation/dehydrogenation cycles were achieved with no sign of deactivation. These results demonstrate the potential of the Ru-PNP/IL system as a Liquid Organic Hydrogen Carrier (LOHC) battery, LOHC H_2 releaser, and hydrogenative CO_2 converter.

INTRODUCTION

Society needs new and sustainable energy solutions to satisfy the growing energy demands. Green hydrogen and Power-to-X technologies will likely be main players in this transition. Carbon capture and utilization (CCU) can lower the world's dependency on fossil resources and contribute to reducing atmospheric greenhouse gas (GHG) levels.[1] At the same time, CCU provides a useful building block for the synthesis of a wide range of industrially relevant chemicals[2,3] and fuels,[4] such as energy carriers as described by Leitner[5] and Olah.[6,7] Arising from CO_2 hydrogenation, formic acid (FA) aspires as a Liquid Organic Hydrogen Carrier (LOHC) for the long-term, safe, and practical storage of hydrogen (4.4 wt% H_2)[8,9] to connect renewable energy and hydrogen fuel cells, potentially closing an ideal carbon-free energy cycle.[10–14] However, employing the CO_2/FA coupled system at low temperatures is a critical feature as fuel cells are intended to provide energy to portable devices with low-heat management profiles. In this sense, developing catalytic systems with high CO_2 hydrogenation efficacy and long-lasting FA dehydrogenation abilities at low temperatures is extremely attractive.

Homogeneous catalyzed hydrogenation and dehydrogenation are two of the main approaches to the reversible interconversion between CO_2 and FA.[10,15–17] However, only a few homogeneous catalyst systems perform in both directions.[18–25] For example, Pidko reported the reversible hydrogenation of CO_2 to formate employing a Milstein Ru-PNP catalyst in DMF/DBU mixtures, demonstrating 10 cycles of H_2 storage-release by only switching the temperature between 65 ºC and 90 ºC as well as the pressure between 5-40 bar and 1 bar.[18] However, the use of relatively volatile solvent and additive render the system impractical for application and scaling up for e.g. rechargeable hydrogen storage and release battery purposes. Hull, Himeda, and Fujita employed a dinuclear iridium catalyst and sacrificial $KHCO_3$ and H_2SO_4 to switch between CO_2 hydrogenation and FA dehydrogenation.[19] The hydrogenation proceeded at 30 ºC under CO_2/H_2 (1:1) at 1 bar, and the dehydrogenation at 50 ºC. Recently, Sponholz, Junge, and Beller developed a triazine-based Mn-PNP complex capable of the reversible CO_2 hydrogenation and FA dehydrogenation when using lysine as stoichiometric additive.[22] Thus, in 1:1 H_2O/THF containing lysine, CO_2 was first trapped from either a pure CO_2 source (2-20 bar) or from air (24 hours at ambient conditions). Then, the FA-lysine adduct is formed by applying 80 bar H_2 at 85 ºC. The H_2 is released again at 90 ºC. Constituting an extremely interesting and promising approach, the procedure nevertheless employs high H_2 pressure and volatile solvents, which both hampers its practical applications.

Despite the interesting properties of the reported methods, none of them are efficient and reversible CO_2/FA catalyst systems that operate under mild conditions and without sacrificial additives (e.g., carbonates, DBU, H_2SO_4) and evasive solvents (e.g. H_2O, DMF, THF)(see SI Table 1). Often the intrinsic nature of the used catalysts requires inert conditions and degassed solutions that represent a further challenge towards practical implementation of the proposed methods. Furthermore, the use of diluted aqueous solutions lowers the volumetric energy storage capacity below practical application. Instead, different strategies for CO_2 valorization to FA[26–35] and for FA dehydrogenation[36–39] have been demonstrated separately. For FA dehydrogenation, even the state-of-the-art catalyst systems require low FA/catalyst ratios, sacrificial additives, and/or volatile solvents to achieve high activity and stability. Hence, as much as efficient catalyst activities are reported, the volumetric and gravimetric FA/H_2 ratios are detrimentally low, leading to unsatisfactory energy storage potentials. In addition, the high levels of volatile solvents (including FA itself) potentially produce H_2 gas containing impurities that are harmful for e.g., a proton-exchange membrane (PEM) fuel cell. On the other hand, a catalytic system that is highly catalytically active and stable at high FA/catalyst ratios in the presence of minimal solvent and no additive would allow for a clean production of H_2 from a continuous flow of FA. Thus, such a system likely represents a viable and practical system for FA-stored H_2 driven transportation.

Ionic liquids (ILs) are a wide family of compounds composed entirely of ions (i.e., salts) and with low melting point. Characteristically, they possess negligible vapor pressure and high chemical and thermal stability, allowing the obtainment of clean H_2 without gaseous contaminants (besides the CO_2) in FA dehydrogenation flow systems. In addition, the high CO_2 uptake capacity of specific ILs[40–44] might render them ideal for CO_2 capture and utilization. However, besides the use of ILs as basic reaction additives, homogeneous complexes operating exclusively in IL as the only solvent are scarcely reported for CO_2/FA systems.[30,32,34] In this work, the IL is envisioned not only to

contribute as a polar solvent with negligible volatility, but also as a base where the basic anion will promote catalyst activation and the imidazolium-derived carbene will work as CO_2 activation agent.

Pincer complexes have been used for a plethora of hydrogenation and dehydrogenation reactions, including the hydrogenation of CO_2 to FA[18,21,22,25-31,33,35] as well as the dehydrogenation of FA for H_2 production.[18,21,22,37,39,45,46]

In this work, we disclose the use of Ru-PNP pincer complexes in ILs for the additive-free, reversible hydrogenation of CO_2 to FA as well as FA dehydrogenation under very mild conditions. The same catalytic system performs both for hydrogenation and dehydrogenation without the need of sacrificial additives showing high compatibility with continuous-flow conditions.

The catalytic system relies on an unprecedented IL-promoted activation of Ru-PNP complexes and allows the hydrogenation of CO_2 to proceed already at 25 °C under 1 bar of CO_2/H_2. Likewise, the release of H_2 from FA occurs at temperatures <100 °C, rendering the catalytic system compatible for PEM fuel cell application. The combination of Ru-PNP complex and IL creates a robust, flexible, and stable catalyst system under a wide range of temperatures, pressures, and catalyst concentrations. The extreme simplicity and stability of the CO_2/FA-based hydrogen storage system further underlines its viable implementation in hydrogen energy technologies. Accordingly, we present a catalytic system that can be applied directly for FA batteries based on reversible CO_2 hydrogenation/FA dehydrogenation,[47] continuous H_2 release from FA as LOHC, as well as a hydrogenative CO_2 converter under energy-efficient conditions.

RESULTS AND DISCUSSION

CO_2 hydrogenation

To achieve the optimal interplay between IL and catalyst, a basic (anion) and imidazolium (cation) based IL capable of trapping CO_2 was combined with a base-activated catalyst that is highly active in facilitating both hydrogenation and dehydrogenation. Thus, initial investigation was performed using the IL 1-ethyl-3-methylimidazolium acetate (EMIM OAc) due to its known ability in chemisorption of CO_2.[44] Satisfyingly, the complex $Ru(H)_2(CO)(^{iPr}PNP)$ (**Ru-1**, 0.02 M, 0.5 mol%) afforded >95% conversion of CO_2 and a TON of >190, corresponding to the formation of FA of 65 mol% compared to the IL (i.e., 65 mol% FA/IL) at 25 ºC after 18 hours of reaction under 10:20 bar pressure of CO_2/H_2 (Table 1, Entry 1). The chlorido (**Ru-2**) and acetato (**Ru-3**) complex analogues showed comparable but inferior results of 70% and 61%, respectively (Entries 2 and 3). Notably, after completion of the reactions using either **Ru-1**, **Ru-2**, or **Ru-3** the main resting species formed was **Ru-3** (SI, Figures 6-9), suggesting that **Ru-2** was activated by the IL during the reaction. Indeed, when **Ru-2** was ex-situ activated by EMIM OAc it formed the same acetato complex **Ru-3** (SI, Figure 10), likely explaining the similar catalytic behavior of the three ^{iPr}PNP complexes.

The catalytic results with alternative PNP-based complexes **Ru-4** (11%), **Ru-5** (36%), and **Ru-6** (<5%) were even more inferior (Entries 4-6), which possibly relates to lower solubility of the complexes in EMIM OAc at 25 °C (observed visually) compared to the ^{iPr}PNP complexes. The higher steric bulk, in particularly when using **Ru-5**, might also play a detrimental role. Other viable hydrogenation catalysts including the ruthenium triphenylphosphine (PPh_3) precursor **Ru-8**, Milstein´s Ru-PNN catalyst **Ru-9** used by Sanford for CO_2 hydrogenation,[48] the Klankermayer-Leitner Ru-Triphos catalyst **Ru-10**,[49] and the Abdur-Rashid Ir-PNP catalyst **Ir-1**,[50] were also evaluated (Entries 8-11). None of the Ru-catalysts afforded NMR-detectable formation of FA under the given reaction conditions while **Ir-1** showed moderate catalytic activity affording 28 mol% FA/IL.

Notably, the system was found highly responsive to variation of the reaction parameters (Table 2). At 25 ºC, the use of elevated H_2 pressure promoted a higher TON, likely because it improves the gas diffusion within the viscous IL-phase that solidifies at 25 ºC when trapping high amounts of CO_2 (Entries 1-6). Loading with 10:20 bar or 15:15 bar of CO_2/H_2 gas mixtures led to similar results (70-75 mol% FA/IL, Entries 4 and 5). Further increasing of the pressure to 20:20 bar of CO_2/H_2 gas resulted in merely 35 mol% FA/IL, with visible formation of unconverted EMIM OAc-CO_2 adduct (Entry 6). Nevertheless, it was possible to reload the system by applying additional 20:20 bar of CO_2/H_2 gas resulting in an over-stoichiometric amount of 126% FA/IL after a second gas charge. Increasing the catalyst loading to 1 mol% (0.04 M) resulted in 92 mol% FA/IL using lower CO_2 pressure (10:20 bar CO_2/H_2, Entry 7), whereas lower catalyst loading of 0.02 mol% (0.0004 M) resulted in only 2 mol% FA/IL and a TON of 280 (Entry 8). Shortening the reaction time to 6 hours using 0.5 mol% of **Ru-1** (0.02 M) led to moderate conversion (30 mol% FA/IL, Entry 9).

The catalytic activity of **Ru-1** in EMIM OAc was also examined at different reaction temperatures. As expected, increasing the reaction temperature from 25 °C to 50 °C or 80 °C led to improved catalytic activities, allowing to decrease the catalyst loading to 0.02-0.05 mol% and 15:15 bar of CO_2/H_2 while maintaining high catalytic activity (Entries 10-14). Moreover, using an increased pressure of 30:30 bar of CO_2/H_2 gas enhanced the gas-diffusion into the IL phase in an up-scaled reaction using 15 mL of EMIM OAc and **Ru-1** (0.0001 M). A TON of 18,886 was reached after 18 hours at 80 ºC, which further increased to 32,411 when additional 30:30 bar of CO_2/H_2 gas was applied for another 18 hours (Entry 15). As a note, the repeated gas loading was only necessary due to the limitations of the equipment, restricting the available gas volume.

To expand on the applicability and robustness of the system, different were examined approaches for the overall hydrogenation process (Scheme 1), including 1) direct reaction, where the CO_2 capture and hydrogenation process occured at the same time in the presence of a CO_2/H_2 gas mixture (reactions **a**-**c**) or 2) a two-step approach where first the CO_2 was captured by the IL followed by subsequent addition of H_2 for the hydrogenation process promoted by the Ru-PNP catalyst (reactions **d**-**f**).

For the direct reactions, the highest FA/IL ratios achieving 130 mol% were obtained using 20:20 bar CO_2/H_2 gas mixture (reaction **a**). Additionally, the catalytic system proved also applicable for preliminary reactions carried out using imitated biogas (i.e., 50:50 vol% CO_2/CH_4) as the CO_2 source. The system afforded a TON of 164 at 50 ºC after 18 hours using 10:20 bar of biogas/H_2 in the presence of **Ru-2** (0.02 M) in EMIM OAc at 50 ºC. Under otherwise identical reaction conditions, **Ru-2** resulted in a TON of 176 and 58 mol% FA/IL using 15:15 bar of biogas/H_2 (reaction **b**). Finally, the possibility of continuous conversion was shown by passing a 1:5 volumetric mixture of CO_2/H_2 gas at 1 bar and 25 ºC through a solution of EMIM OAc containing **Ru-1** (0.07 M) to achieve 14 mol% FA/IL (TON of 15) after 96 hours (reaction **c**).

In the two-step CO_2 hydrogenation process, initial charging of 25 bar of CO_2 to EMIM OAc (2 mL) and **Ru-2** (0.01 M) for 45 minutes at 25 °C results in 34 mol% CO_2/IL. Subsequent release of the CO_2 pressure and addition of 25 bar of H_2 afforded 60 mol% FA/IL (TON of 359) after 18 hours at 50 ºC (reaction **d**). Likely, remnants of non-chemisorbed gaseous CO_2 in the IL accounted for the discrepancy between the amount of trapped CO_2 and FA yield. In a similar fashion, when passing firstly CO_2 through EMIM OAc (2 mL) for 48 hours under ambient conditions (25 °C) a solid

precipitate was obtained due to the accumulation of EMIM OAc-CO_2. The solid mixture was then loaded with **Ru-2** (0.02 mmol) and 25 bar of H_2 gas at 50 ºC resulting in 38 mol% FA/IL (Scheme 1, reaction **e**). A final experiment was performed passing directly 1 bar CO_2 gas through EMIM OAc (1.5 mL) at 25 ºC, which yielded 10 mol% of CO_2 trapped after 24 hours. Addition of **Ru-1** (0.02 mmol) and switching the atmosphere to H_2 with a balloon at ambient conditions resulted in 12 mol% of FA/IL (TON of 58) after 96 hours (reaction **f**). Importantly, all the above-mentioned manipulations were performed under non-inert conditions.

Table 1. Screening of catalysts for the hydrogenation of CO2 to FA.

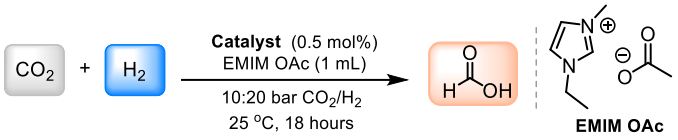

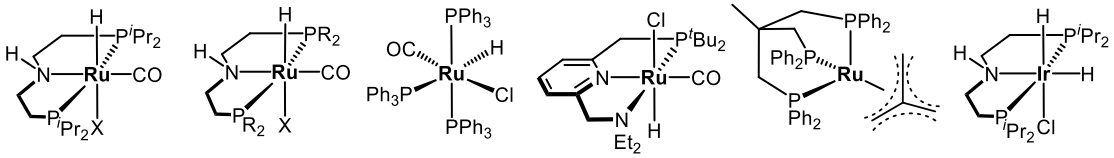

Entry[a]	Catalyst	TON	TOF [h^{-1}]	FA yield[b] [%]	FA/IL[c] [mol%]
1	**Ru-1**	>190	10	>95	65
2	**Ru-2**	135	8	70	42
3	**Ru-3**	109	6	61	36
4	**Ru-4**	22	2	11	7
5	**Ru-5**	66	4	36	22
6	**Ru-6**	-	-	<5	<5
7	**Ru-7**	-	-	<5	<5
8	**Ru-8**	-	-	<5	<5
9	**Ru-9**	-	-	<5	<5
10	**Ru-10**	-	-	<5	<5
11	**Ir-1**	81	4	36	28

[a] 0.02 mmol catalyst (0.5 mol% compared to CO_2), EMIM OAc (1 mL), 10:20 bar of CO_2/H_2, 25 ºC, 18 hours.
[b] Determined by ^1H NMR (calculated from amount of CO_2).
[c] Determined by ^1H NMR. Reactions reproducible within an error margin of 10%.

Performing the reaction using D_2 and $^{13}CO_2$ in the presence of EMIM OAc and **Ru-2** corroborated that CO_2 hydrogenation occured along with IL-based imidazoline formation and that FA indeed arised from the CO_2 (Scheme 2 and SI Figures 11-15). Thus, the ^2H NMR spectrum of the reaction mixture with D_2 showed the presence of deuterium-labels of FA at δ = 8.60 ppm and of the C2 position of the IL imidazolium ion at δ = 9.55 ppm (Scheme 2, reaction 1). The ^{13}C NMR spectrum of reaction 2 showed the presence of ^{13}C-labeled FA at δ = 166 ppm accompanied by the splitting of the signal due to coupling with a proton. Likewise, the peak at δ = 155 ppm was assigned to the imidazolium carboxylate species ^{13}C-labeled on the carboxylate arising from the imidazoline reacting with $^{13}CO_2$.

Scheme 2. Labelling studies with D_2 and $^{13}CO_2$ of CO_2 hydrogenation to FA in IL.

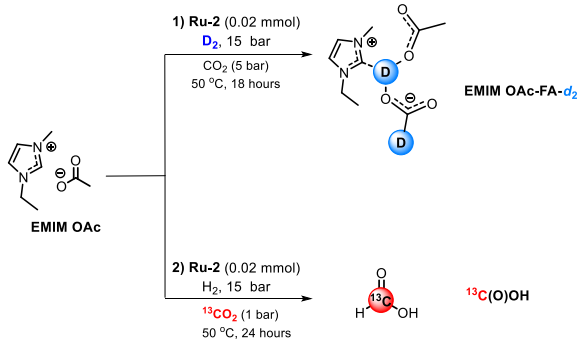

Table 2. Screening of reaction conditions for the hydrogenation of CO_2 at mild conditions using Ru-1 and EMIM OAc.

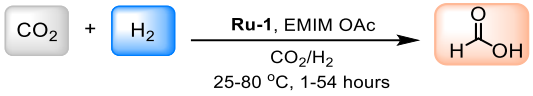

Entry	**Ru-1** conc. [M]	**Ru-1** loading [mol%][a]	CO_2/H_2 [bar]	T [°C]	Time [h]	TON	TOF [h^{-1}]	FA/IL[b] [mol%]
1	0.02	0.6	5:5	25	18	16	-	5
2	0.02	0.6	5:10	25	18	26	-	8
3	0.02	0.5	10:10	25	18	71	4	22
4	0.02	0.5	10:20	25	18	198	10	75
5	0.02	0.2	15:15	25	18	184	10	70
6	0.02	-	20:20	25	54	405	7	126
7	0.04	1.0	10:20	25	18	141	8	92
8	0.004	0.02	15:15	25	18	280	15	2
9	0.02	0.5	10:20	25	6	92	15	30
10	0.002	0.05	15:15	50	18	1,515	84	47
11	0.004	0.05	15:15	80	1	258	258	16
12	0.004	0.05	15:15	80	6	1,052	175	65
13	0.002	0.05	15:15	80	18	1,935	107	60
14	0.0004	0.02	15:15	80	18	3,085	171	22
15[c]	0.0001	-	30:30	80	36	32,411	900	67

a Mol% refers to amount of CO_2. Not determined in Entries 6 and 15.
b Determined by ^1H NMR. Reactions reproducible within an error margin of 10%.
c Reloaded with 30:30 bar CO_2/H_2 after 18 hours.

Scheme 1. Different approaches for CO_2 capture and hydrogenation to FA in one- and two steps in a Ru-2/EMIM OAc system.

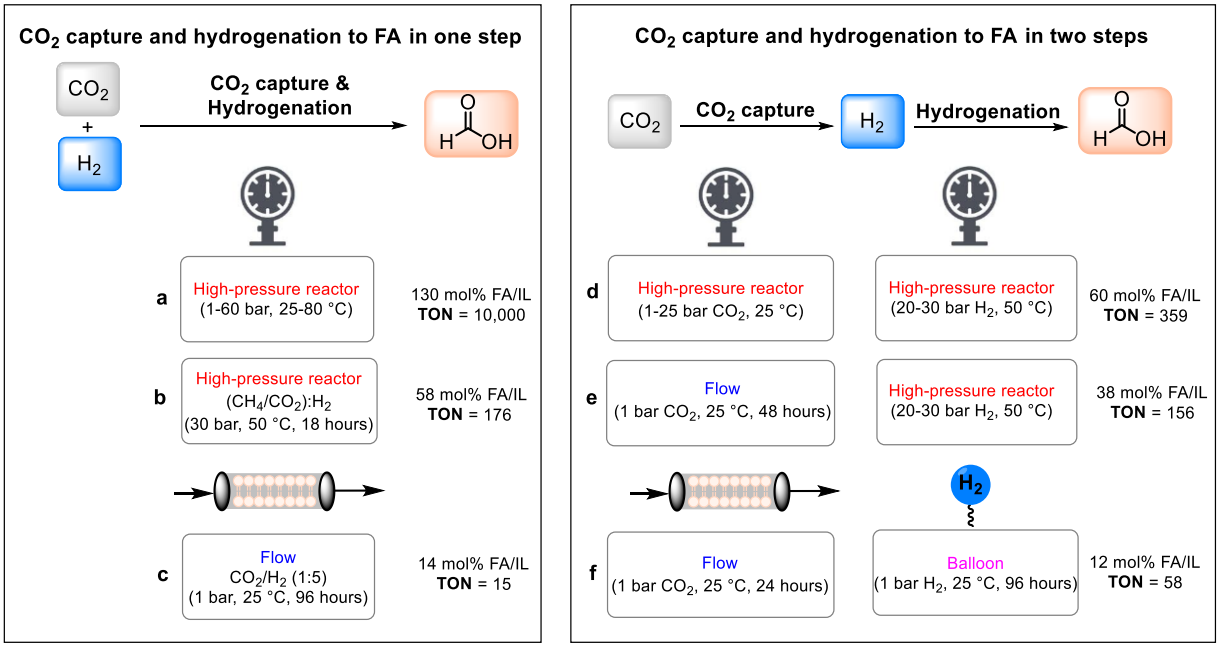

Formic Acid dehydrogenation

The reverse reaction (i.e., FA dehydrogenation) was next explored with batch studies commencing with BMIM OAc due to its low propensity towards CO_2 capture that could affect the gas release and thus the catalytic performance (Table 3). The catalysts **Ru-1**, **Ru-2**, **Ru-3**, **Ru-6**, and **Ru-7** (0.1 mol%) all reached full conversion within 2 hours (Entries 1-5) with no clear difference observed between BMIM OAc and EMIM OAc (Entry 5 and 6, respectively).

After completion of the reaction, IL-trapped CO_2 and the **Ru-3** complex were observed when using **Ru-1** as the catalyst (SI, Figure 16). Lowering the catalyst loading of **Ru-7** four-fold to 0.025 mol% leads to a higher TON of 3,780 (Entry 7), whereas increased loading of FA (53 mmol) resulted in poor activity and deactivation of the catalyst (Entry 8). This suggested that a high FA loading required more IL to balance the increased acidity of the mixture and/or presence of carboxylic acid. In fact, a TON of 12,050 was obtained at 95 ºC after 18 hours with 0.007 mol% of **Ru-7** in 3 mL of BMIM OAc instead of the 1 mL otherwise used (Entry 9). In a similar experiment, two aliquots (26.5 mmol) of FA were added at different times resulting in an overall TON of 16,750 (Entry 10). Importantly, no CO gas was detected (detection limit <100 ppm) under the applied reaction conditions (SI, Figure 25), and fast gas evolution immediately occurred upon FA addition in a typical batch experiment until all FA was consumed. The same behavior was observed when more FA was subsequently added (SI, Figure 17). Hence, the reaction was highly dependent on the FA addition rate, suggesting that high TONs and TOFs were possible when keeping the IL/FA ratio at an optimal level. Finally, it was noticed that the mixture containing **Ru-6** and BMIM OAc (Entry 1) was still active after 4 weeks of simple storage under ambient conditions and retained the same catalytic activity reaching full conversion when more FA (13.25 mmol) was added at 80 ºC. These findings inspired to an evaluation of the durability of the catalytic system with continuous FA feed, simulating an application such as automotive fuel cell technologies.

Thus, at 80 ºC the **Ru-7** (0.047 mmol) in BMIM OAc (2 mL) indeed allowed for a FA feed rate of up to 5 mL/h (TOF of 2,820 h^{-1}) while up to 10 mL/h (TOF of 10,600 h^{-1}) was tolerated at 95 ºC using less catalyst loading (0.025 mmol of **Ru-7**, SI, Table 3). **Ru-1** and **Ru-2** (0.02 mmol, 0.01 M) reached a TOF_{max} of 7,288 h^{-1} with a maximum feeding rate of 5.5 mL/h. **Ru-6** showed similar results as its ^{Ph}PNP congener **Ru-7** affording a TOF_{max} of 10,800 h^{-1} equal to a FA rate of 10 mL/h. Based on these results, the optimization of the system was continued using the thermally more labile complex **Ru-7** containing the -HBH_3 ligand. In addition, a superior stability over time was found of the ^{Ph}PNP pincer in the presence of FA compared to the ^{iPr}PNP analogues. As seen in Figure 18 (SI), the system readily dehydrogenated all the FA from any feeding rates within the maximum tolerated rate.

Table 3. Screening of catalysts and optimization of FA dehydrogenation in batch conditions using BMIM OAc.

Entry	Catalyst	Catalyst concentration [M]	Catalyst loading [mol%]	TON	TOF [h^{-1}]	Conversion [%][a]
1	**Ru-6**	0.01	0.1	1,000	500	>99
2	**Ru-2**	0.01	0.1	1,000	500	>99
3	**Ru-3**	0.01	0.1	1,000	500	>99
4	**Ru-1**	0.01	0.1	1,000	500	>99
5	**Ru-7**	0.01	0.1	1,000	500	>99
6[b]	**Ru-7**	0.01	0.1	1,000	500	>99
7	**Ru-7**	0.003	0.25	3,780	1,260	>99
8[c]	**Ru-7**	0.003	0.006	-	-	-
9[d]	**Ru-7**	0.001	0.007	12,050	502	90
10[e]	**Ru-7**	0.001	0.005	16,750	930	95

Reaction conditions: A given amount of catalyst in BMIM OAc (1 mL, 6 mmol) and FA (0.5 mL, 13.25 mmol) at 80 °C for 3 hours. Gas evolution is followed by mass flow meter (MFM) and gas composition is analysed by Micro-GC.

[a] Determined by ^{1}H NMR.

[b] EMIM OAc (1 mL, 7 mmol).

[c] **Ru-7** (0.003 mmol), FA (2 mL, 53 mmol).

[d] **Ru-7** (0.003 mmol), BMIM OAc (3 mL, 18.5 mmol), FA (1.5 mL, 39.8 mmol), 95 ºC, 18 hours.

[e] **Ru-7** (0.003 mmol), BMIM OAc (3 mL, 18.5 mmol), FA (1 x 2 mL, 26.5 x 2 mmol), 95 ºC, 18 hours (second addition of FA after 5 hours).

Figure 1. Gas evolution profile of continuous-flow addition of FA to Ru-7 in BMIM OAc.

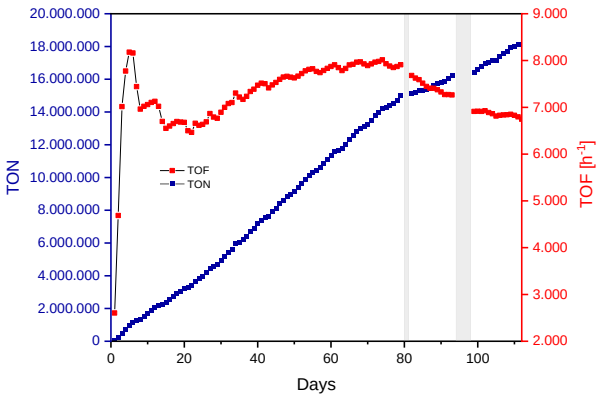

Lowering the catalyst concentration from 0.01 to 0.005 M resulted in a stabilizing buffering effect of the IL towards the increasing acidity of the solution given by higher FA rates (SI, Table 4). In a final long-term experiment, **Ru-7** (0.005 M, 0.02 mmol) in BMIM OAc (4 mL) dehydrogenated 14.5 L of FA at 95 ºC, resulting in a TON of 18,100,000 after 112 days (Figure 1), corresponding to a volume ratio between FA and IL of >3,600. The maximum FA feed rate was set to 8.4 mL/h corresponding to a TOF of 11,134 h^{-1}. Noteworthy, after 79 days a decrease in the gas flow along with accumulation of FA was observed (Figure 1, first gray bar in the graph). The excess FA was removed, which allowed to restart the reaction albeit only at 75% catalytic activity, as the FA feed rate decreased from 8 mL/h to 6 mL/h. This behavior might be explained by accumulation of water and/or salt impurities that are present in the commercial grade FA. Afterwards, the system remained stable until day 112 when the reaction was stopped (maximum FA rate of 6 mL/h, 160 mL/min gas flow, overall TOF of 7,194 h^{-1} over the 112 days). It was possible to pause the system for at least 4 days, during which it was cooled to 25 ºC before heated up again to 95 ºC and restoring the FA feed (Figure 1, second gray bar in the graph). Notably, ^{1}H NMR analysis of the post-reaction system revealed that the acetate anion was completely replaced by formate during the 112 days of reaction, resulting in the formation of BMIM CHOO (SI, Figure 24). No CO gas formation was detected by periodic measurements over the 108 days (SI, Figure 26).

The obtained results significantly exceed previously reported catalytic systems for homogeneous FA dehydrogenation in terms of activity and durability as well as volume ratio between consumed FA and reactor size. Thus, as opposed to classical batch type reactions where FA is added initially in large amounts, a versatile and small-volume unit is here demonstrated that simulates the conditions of, for example, a hydrogen vehicle. In a practical perspective, all the manipulations were carried out under ambient conditions, using commercial grade FA without prior purification, demonstrating the feasibility of using neat FA to reach the maximum gravimetric H_2 content of the system, improving its energetic and volumetric properties in a reduced scale.

CO_2 hydrogenation / FA dehydrogenation cycles

It is possible to shift the equilibrium in the catalytic system towards the hydrogenation or dehydrogenation by controlling either the pressure or the temperature. By applying heat (>60 ºC) to a FA/IL mixture, a release of a 1:1 mixture of CO_2/H_2 gas was detected. Thus, by applying a pressure switch from CO_2/H_2 gas mixture load and readily releasing H_2 gas from the reaction at constant temperature (80 ºC) an overall TON of 51,761 resulted after 10 cycles with no indication of catalyst deactivation with **Ru-1** (0.0013 M) in EMIM OAc (SI, Figure 20). Similarly, the hydrogenation step could be performed over 18 hours or 72 hours at 25 ºC under 10:20 bar of CO_2/H_2, while the H_2 gas release was favored by heating to 95 ºC for 4 hours (Figure 2). Both **Ru-1** and **Ru-2** catalyzed 13 reaction cycles without observable loss of catalytic activity. No further cycles were attempted. For **Ru-1** (0.07 mmol, 0.035 M), each hydrogenation step plateaued at approximately 70 mol% FA/IL, while lower concentration of **Ru-2** (0.05 mmol, 0.025 M) produced even higher FA/IL molar ratios (>100 mol%) affording an overall TON of 7,739 after 13 cycles of charge and discharge (SI, Figure 21). Importantly, it was also possible to achieve the H_2 gas release step in a closed system. In such fashion, a detected pressure of at least 10 bars of H_2 can be achieved in a single dehydrogenation step, though much higher pressures (>100 bar) in principle could be obtained as well. However, a significant amount of CO was detected under such operation.

Figure 2. Cycles applied to CO_2 hydrogenation experiments followed by hydrogen release.

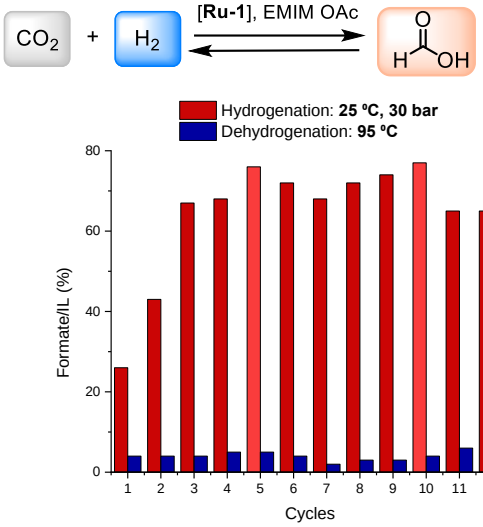

Mechanism

Suggested catalytic cycles for both directions of CO_2 hydrogenation to FA and FA dehydrogenation to CO_2 and H_2 are illustrated in Scheme 3. For the CO_2 hydrogenation (red catalytic cycle), the imidazoline **a** first formed by an acid/base reaction between the IL imidazolium cation and acetate anion. Interaction of **a** with CO_2 led to the imidazolium carboxylate **b**. Simultaneously, the Ru-PNP precatalyst was activated by the IL. Complexes **Ru-3a** and **Ru-3b** were likely the main resting species, and they were in equilibrium with **Ru-1** when under H_2 pressure. **Ru-1** then interacted with **b** leading to intermediate **Ru-1-b**. Hydride transfer of the ruthenium hydrido to the carboxylate carbon followed by dissociation of FA restored **a**, which could take up a new molecule of CO_2. **Ru-11**, formed from the hydrogen transfer, was re-hydrogenated to regenerate **Ru-1**. Simultaneously, the more basic acetate deprotonated FA leading to formate and acetic acid.

For the FA dehydrogenation (blue catalytic cycle), **Ru-3a** and **Ru-3b** also constitute the main resting species. They were in equilibrium with **Ru-11**, which interacted with FA providing intermediate **Ru-11-FA**. Collapse of the coordinating FA in **Ru-11-FA** was promoted by hydrogen-bonding of the IL acetate anion to the proton residing between the amido and FA, which renders

the partially negatively charged FA more electron-rich and thus more prone to deliver the hydride. Following the hydride deliver, CO_2 and **Ru-1** were formed. Finally, extrusion of H_2 regenerated **Ru-11**, which is ready for a new catalytic cycle.

CONCLUSIONS

This work demonstrates a new homogeneous catalytic approach for the hydrogenation of CO_2 to FA and the reverse FA dehydrogenation based on Ru-PNP complexes in IL. The catalytic system showed high activity and stability in CO_2 hydrogenation already under ambient conditions (25 ºC, 1 bar), and the dehydrogenation of FA proceeded TOFs exceeding 10,000 h^{-1} at 95 ºC, a temperature that is compatible with PEM fuel cell applications. The system remained active for dehydrogenation of a continuous flow of FA for up to 4 months, achieving an overall TON exceeding 18 million, the best result to date in terms of both catalyst activity and stability. Moreover, no contamination of organic residues nor CO was observed in the gas stream, and the system was prone to catalyzing at least 13 cycles of hydrogenation/dehydrogenation with no detectable loss of catalytic activity. Switching between the cycles was favored by simply changing either pressure or temperature conditions.

The introduced catalyst system shows extreme flexibility, stability, and reversibility under a wide range of temperatures, pressures, operating times, and catalyst loadings. All these features render the system a promising candidate for energy storage technologies based on H_2-FA presenting practical advantages such as storage and easy manipulations under ambient conditions, as well as the possibility to dehydrogenate neat FA maximizing the atom efficiency and hydrogen gravimetric content of the system. It is possible to pause and stop the system, which could potentially be positioned in a small compartment with non-heated liquid FA added continuously from a separate container. Indeed, this likely represent the ideal conditions for practical implementation of the technology for low-temperature hydrogen release compatible with fuel cell technologies within the transportation sector.

Scheme 3. Suggested mechanisms for the Ru-PNP catalyzed CO_2 hydrogenation to FA (left catalytic cycle) and the Ru-PNP catalyzed FA dehydrogenation to CO_2 and H_2 (right catalytic cycle). The activation of CO_2 by imidazoline in EMIM OAc is also shown (above left catalytic cycle).

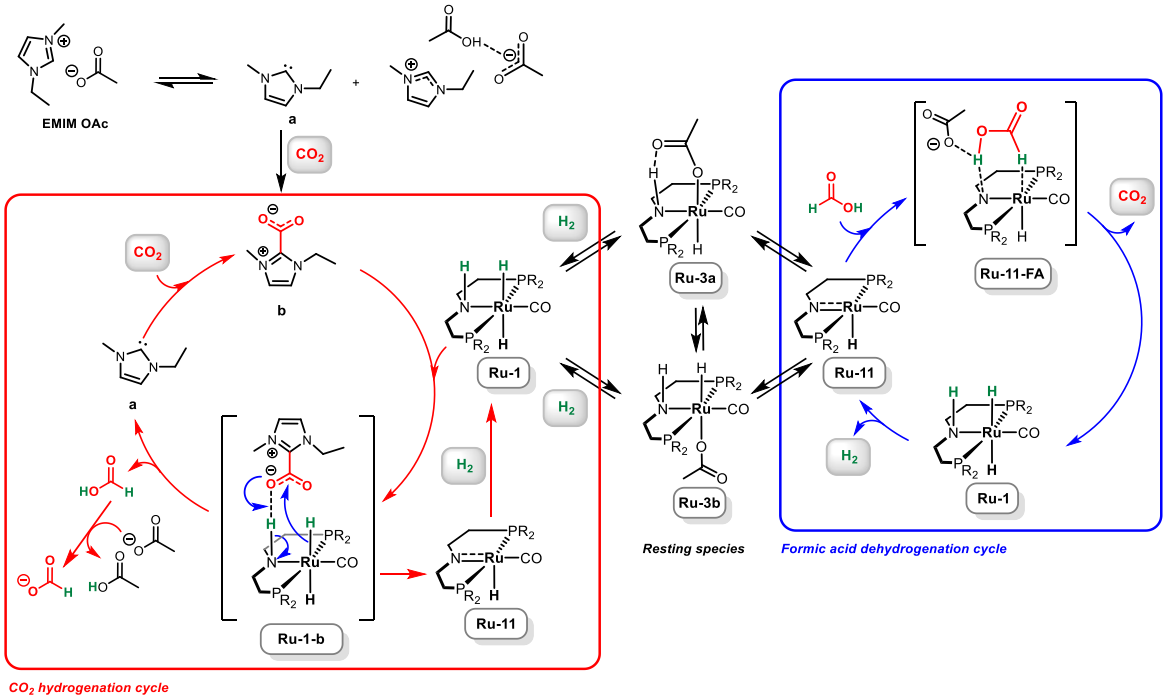

ASSOCIATED CONTENT

(Word Style "TE_Supporting_Information"). **Supporting Information**. A brief statement in nonsentence format listing the contents of material supplied as Supporting Information should be included, ending with "This material is available free of charge via the Internet at http://pubs.acs.org." For instructions on what should be included in the Supporting Information as well as how to prepare this material for publication, refer to the journal's Instructions for Authors.

AUTHOR INFORMATION

Corresponding Author

* Shoubhik Das, shoubhik.das@uantwerpen.be; Tel.: +32-653226
* Martin Nielsen, marnie@kemi.dtu.dk; Tel.: +45-24651045

Funding Sources

The authors are grateful at the VILLUM FONDEN (19049), Carlsberg Foundation (CF20-0365), Independent Research Fund Denmark (8022-00330B), Novo Nordisk Foundation (NNF20OC0064560), COWI Foundation (A-149.10), and Brødrene Hartmanns Foundation (A32.745). MN and SD thank Independent Research Fund Denmark (1127-00172B) for generous funding. AR thanks Novo Nordisk Foundation (NNF21OC0072015). LP thanks Otto Mønsted (22-55-0557), Brødrene Hartmanns Foundation (A37.412), and DTU Discovery Grant.

ACKNOWLEDGMENT

We thank Kasper Enemark-Rasmussen, Department of Chemistry, Technical University of Denmark, for carrying out a range of NMR measurements.

REFERENCES

(1) Sabri, M. A.; Al Jitan, S.; Bahamon, D.; Vega, L. F.; Palmisano, G. Current and Future Perspectives on Catalytic-Based Integrated Carbon Capture and Utilization. *Sci. Total Environ.* **2021**, *790*, 148081.

(2) Zhang, Z.; Pan, S.-Y.; Li, H.; Cai, J.; Olabi, A. G.; Anthony, E. J.; Manovic, V. Recent Advances in Carbon Dioxide Utilization. *Renewable Sustainable Energy Rev.* **2020**, *125*, 109799.

(3) Dabral, S.; Schaub, T. The Use of Carbon Dioxide (CO 2) as a Building Block in Organic Synthesis from an Industrial Perspective. *Adv. Synth. Catal.* **2019**, *361* (2), 223–246.

(4) Centi, G.; Perathoner, S. Opportunities and Prospects in the Chemical Recycling of Carbon Dioxide to Fuels. *Catal. Today* **2009**, *148* (3–4), 191–205.

(5) Leitner, W. Carbon Dioxide as a Raw Material: The Synthesis of Formic Acid and Its Derivatives from CO_2. *Angew. Chem. Int. Ed.* **1995**, *34*, 2207–2221.

(6) Olah, G. A. Beyond Oil and Gas: The Methanol Economy. *Angew. Chem. Int. Ed.* **2005**, *44*, 2636–2639.

(7) Olah, G. A.; Goeppert, A.; Prakash, G. K. S. The "Methanol Economy": General Aspects. In *Beyond Oil and Gas*; 2018.

(8) Müller, K.; Brooks, K.; Autrey, T. Hydrogen Storage in Formic Acid: A Comparison of Process Options. *Energy & Fuels* **2017**, *31*, 12603–12611.

(9) Guo, J.; Yin, C. K.; Zhong, D. L.; Wang, Y. L.; Qi, T.; Liu, G. H.; Shen, L. T.; Zhou, Q. S.; Peng, Z. H.; Yao, H.; Li, X. B. Formic Acid as a Potential On-Board Hydrogen Storage Method: Development of Homogeneous Noble Metal Catalysts for Dehydrogenation Reactions. *ChemSusChem* **2021**, *14*, 2655–2681.

(10) Sordakis, K.; Tang, C.; Vogt, L. K.; Junge, H.; Dyson, P. J.; Beller, M.; Laurenczy, G. Homogeneous Catalysis for Sustainable Hydrogen Storage in Formic Acid and Alcohols. *Chem. Rev.* **2018**, *118*, 372–433.

(11) Mellmann, D.; Sponholz, P.; Junge, H.; Beller, M. Formic Acid as a Hydrogen Storage Material-Development of Homogeneous Catalysts for Selective Hydrogen Release. *Chem. Soc. Rev.* **2016**, *45*, 3954–3988.

(12) Loges, B.; Boddien, A.; Gärtner, F.; Junge, H.; Beller, M. Catalytic Generation of Hydrogen from Formic Acid and Its Derivatives: Useful Hydrogen Storage Materials. *Top. Catal.* **2010**, *53*, 902–914.

(13) Ma, Z.; Legrand, U.; Pahija, E.; Tavares, J. R.; Boffito, D. C. From CO_2 to Formic Acid Fuel Cells. *Ind. Eng. Chem. Re.s* **2021**, *60*, 803–815.

(14) van Putten, R.; Wissink, T.; Swinkels, T.; Pidko, E. A. Fuelling the Hydrogen Economy: Scale-up of an Integrated Formic Acid-to-Power System. *Int. J. Hydrog. Energy* **2019**, *44*, 28533–28541.

(15) Sancho-Sanz, I.; Korili, S. A.; Gil, A. Catalytic Valorization of CO_2 by Hydrogenation: Current Status and Future Trends. *Catal. Rev. Sci. Eng.* **2021**, DOI: 10.1080/01614940.2021.1968197

(16) Kumar, A.; Daw, P.; Milstein, D. Homogeneous Catalysis for Sustainable Energy: Hydrogen and Methanol Economies, Fuels from Biomass, and Related Topics. *Chem. Rev.* **2021**, *122*, 385-441.

(17) Piccirilli, L.; Lobo Justo Pinheiro, D.; Nielsen, M. Recent Progress with Pincer Transition Metal Catalysts for Sustainability. *Catalysts* **2020**, *10*, 773.

(18) Filonenko, G. A.; van Putten, R.; Schulpen, E. N.; Hensen, E. J. M.; Pidko, E. A. Highly Efficient Reversible Hydrogenation of Carbon Dioxide to Formates Using a Ruthenium PNP-Pincer Catalyst. *ChemCatChem* **2014**, *6*, 1526–1530.

(19) Hull, J. F.; Himeda, Y.; Wang, W.-H.; Hashiguchi, B.; Periana, R.; Szalda, D. J.; Muckerman, J. T.; Fujita, E. Reversible Hydrogen Storage Using CO2 and a Proton-Switchable Iridium Catalyst in Aqueous Media under Mild Temperatures and Pressures. *Nat. Chem.* **2012**, *4*, 383–388.

(20) Onishi, N.; Kanega, R.; Fujita, E.; Himeda, Y. Carbon Dioxide Hydrogenation and Formic Acid Dehydrogenation Catalyzed by Iridium Complexes Bearing Pyridyl-Pyrazole Ligands: Effect of an Electron-Donating Substituent on the Pyrazole Ring on the Catalytic Activity and Durability. *Adv. Synth. Catal.* **2019**, *361*, 289–296.

(21) Kothandaraman, J.; Czaun, M.; Goeppert, A.; Haiges, R.; Jones, J.; May, R.; Prakash, G.; Olah, G. Amine-free reversible hydrogen storage in formate salts catalyzed by ruthenium pincer complex without pH control or solvent change. *ChemSusChem* **2015**, 8, 1442-1451.

(22) Wei, D.; Sang, R.; Sponholz, P.; Junge, H.; Beller, M. Reversible hydrogenation of carbon dioxide to formic acid using a Mn-pincer complex in the presence of lysine. *Nat. Energy* **2022**, *7*, 438-447.

(23) Tsai, H.; Lien, W.; Liao, C.; Chen, Y.; Huang, S.; Chou, F.; Chang, C.; Yu, J.; Kao, Y.; Wu, T. Efficient and Reversible Catalysis of Formic Acid-Carbon Dioxide Cycle Using Carbamate-Substituted Ruthenium-Dithiolate Complexes. *ChemCatChem* **2021**, *13*, 4092-4098.

(24) Hsu, S.; Rommel, S.; Eversfield, P.; Muller, K.; Klemm, E.; Thiel, W.; Plietker, B. A Rechargeable Hydrogen Battery Based on Ru Catalysis. *Angew. Chem. Int. Ed.* **2014**, *53*, 7074-7078.

(25) Tanaka, R.; Yamashita, M.; Chung, L.; Morokuma, K.; Nozaki, K. Mechanistic Studies on the Reversible Hydrogenation of Carbon Dioxide Catalyzed by an Ir-PNP Complex. *Organometallics* **2011**, *30*, 6742-6750.

(26) Zhang, Y.; MacIntosh, A. D.; Wong, J. L.; Bielinski, E. A.; Williard, P. G.; Mercado, B. Q.; Hazari, N.; Bernskoetter, W. H. Iron Catalyzed CO2 Hydrogenation to Formate Enhanced by Lewis Acid Co-Catalysts. *Chem. Sci.* **2015**, *6*, 4291–4299.

(27) Kar, S.; Goeppert, A.; Galvan, V.; Chowdhury, R.; Olah, J.; Prakash, G. K. S. A Carbon-Neutral CO_2 Capture, Conversion, and Utilization Cycle with Low-Temperature Regeneration of Sodium Hydroxide. *J. Am. Chem. Soc.* **2018**, *140*, 16873–16876.

(28) Kar, S.; Goeppert, A.; Prakash, G. K. S. Integrated CO2 Capture and Conversion to Formate and Methanol: Connecting Two Threads. *Acc. Chem. Res.* **2019**, *52*, 2892–2903.

(29) Wang, W. H.; Himeda, Y.; Muckerman, J. T.; Manbeck, G. F.; Fujita, E. CO_2 Hydrogenation to Formate and Methanol as an Alternative to Photo- and Electrochemical CO_2 Reduction. *Chem. Rev.* **2015**, *115*, 12936–12973.

(30) Weilhard, A.; Argent, S. P.; Sans, V. Efficient Carbon Dioxide Hydrogenation to Formic Acid with Buffering Ionic Liquids. *Nat. Commun.* **2021**, *12*, 1–7.

(31) Kothandaraman, J.; Goeppert, A.; Czaun, M.; Olah, G. A.; Surya Prakash, G. K. CO_2 Capture by Amines in Aqueous Media and Its Subsequent Conversion to Formate with Reusable Ruthenium and Iron Catalysts. *Green Chem.* **2016**, *18*, 5831–5838.

(32) Wesselbaum, S.; Hintermair, U.; Leitner, W. Continuous-Flow Hydrogenation of Carbon Dioxide to Pure Formic Acid Using an Integrated $ScCO_2$ Process with Immobilized Catalyst and Base. *Angew. Chem. Int. Ed.* **2012**, *51*, 8585–8588.

(33) Tanaka, R.; Yamashita, M.; Nozaki, K. Catalytic Hydrogenation of Carbon Dioxide Using Ir(III)-Pincer Complexes. *J. Am. Chem. Soc.* **2009**, *131*, 14168–14169.

(34) Weilhard, A.; Qadir, M. I.; Sans, V.; Dupont, J. Selective CO_2 Hydrogenation to Formic Acid with Multifunctional Ionic Liquids. *ACS Catal.* **2018**, *8*, 1628–1634.

(35) Liu, Q.; Wu, L.; Gülak, S.; Rockstroh, N.; Jackstell, R.; Beller, M. Towards a Sustainable Synthesis of Formate Salts: Combined

Catalytic Methanol Dehydrogenation and Bicarbonate Hydrogenation. *Angew. Chem. Int. Ed.* **2014**, *53*, 7085–7088.
(36) Boddien, A.; Mellmann, D.; Gärtner, F.; Jackstell, R.; Junge, H.; Dyson, P.; Laurenczy, G.; Ludwig, R.; Beller, M. Efficient Dehydrogenation of Formic Acid Using an Iron Catalyst. *Science* **2011,** *333*, 1733-1736.
(37) Kar, S.; Rauch, M.; Leitus, G.; Ben-David, Y.; Milstein, D. Highly Efficient Additive-Free Dehydrogenation of Neat Formic Acid. *Nat. Catal.* **2021**, *4*, 193–201.
(38) Bielinski, E. A.; Lagaditis, P. O.; Zhang, Y.; Mercado, B. Q.; Würtele, C.; Bernskoetter, W. H.; Hazari, N.; Schneider, S. Lewis Acid-Assisted Formic Acid Dehydrogenation Using a Pincer-Supported Iron Catalyst. *J. Am. Chem. Soc.* **2014**, *136*, 10234–10237.
(39) Onishi, N.; Kanega, R.; Kawanami, H.; Himeda, Y. Recent Progress in Homogeneous Catalytic Dehydrogenation of Formic Acid. *Molecules* **2022**, *27*, 455.
(40) Aghaie, M.; Rezaei, N.; Zendehboudi, S. A Systematic Review on CO_2 Capture with Ionic Liquids: Current Status and Future Prospects. *Renewable Sustainable Energy Rev.* **2018**, *96*, 502–525.
(41) Torralba-Calleja, E.; Skinner, J.; Gutiérrez-Tauste, D. CO_2 Capture in Ionic Liquids: A Review of Solubilities and Experimental Methods. *J. Chem.* **2013**, *2013*, Article ID 473584.
(42) Ramdin, M.; de Loos, T. W.; Vlugt, T. J. H. State-of-the-Art of CO_2 Capture with Ionic Liquids. *Ind. Eng, Chem, Re,s* **2012**, *51*, 8149–8177.
(43) Shukla, S. K.; Khokarale, S. G.; Bui, T. Q.; Mikkola, J.-P. T. Ionic Liquids: Potential Materials for Carbon Dioxide Capture and Utilization. *Front. Mater.* **2019**, *6*, 1–8.
(44) Gurau, G.; Rodríguez, H.; Kelley, S. P.; Janiczek, P.; Kalb, R. S.; Rogers, R. D. Demonstration of Chemisorption of Carbon Dioxide in 1,3-Dialkylimidazolium Acetate Ionic Liquids. *Angew. Chem. Int. Ed.* **2011**, *50*, 12024–12026.
(45) Agapova, A.; Alberico, E.; Kammer, A.; Junge, H.; Beller, M. Catalytic Dehydrogenation of Formic Acid with Ruthenium-PNP-Pincer Complexes: Comparing N-Methylated and NH-Ligands. *ChemCatChem* **2019**, *11*, 1910–1914.
(46) Iguchi, M.; Himeda, Y.; Manaka, Y.; Kawanami, H. Development of an Iridium-Based Catalyst for High-Pressure Evolution of Hydrogen from Formic Acid. *ChemSusChem* **2016**, *9*, 2749–2753.
(47) Wei, D.; Sang, R.; Moazezbarabadi, A.; Junge, H.; Beller, M. Homogeneous Carbon Capture and Catalytic Hydrogenation: Toward a Chemical Hydrogen Battery System. *JACS Au* **2022**, *2*, 1020–1031.
(48) Huff, C. A.; Sanford, M. S. Catalytic CO_2 Hydrogenation to Formate by a Ruthenium Pincer Complex. *ACS Catal.* **2013**, *3*, 2412–2416.
(49) Wesselbaum, S.; Moha, V.; Meuresch, M.; Brosinski, S.; Thenert, K. M.; Kothe, J.; Stein, T. Vom; Englert, U.; Hölscher, M.; Klankermayer, J.; Leitner, W. Hydrogenation of Carbon Dioxide to Methanol Using a Homogeneous Ruthenium-Triphos Catalyst: From Mechanistic Investigations to Multiphase Catalysis. *Chem. Sci.* **2015**, *6*, 693–704.
(50) Clarke, Z. E.; Maragh, P. T.; Dasgupta, T. P.; Gusev, D. G.; Lough, A. J.; Abdur-Rashid, K. A Family of Active Iridium Catalysts for Transfer Hydrogenation of Ketones. *Organometallics* **2006**, *25*, 4113–4117.

Insert Table of Contents artwork here

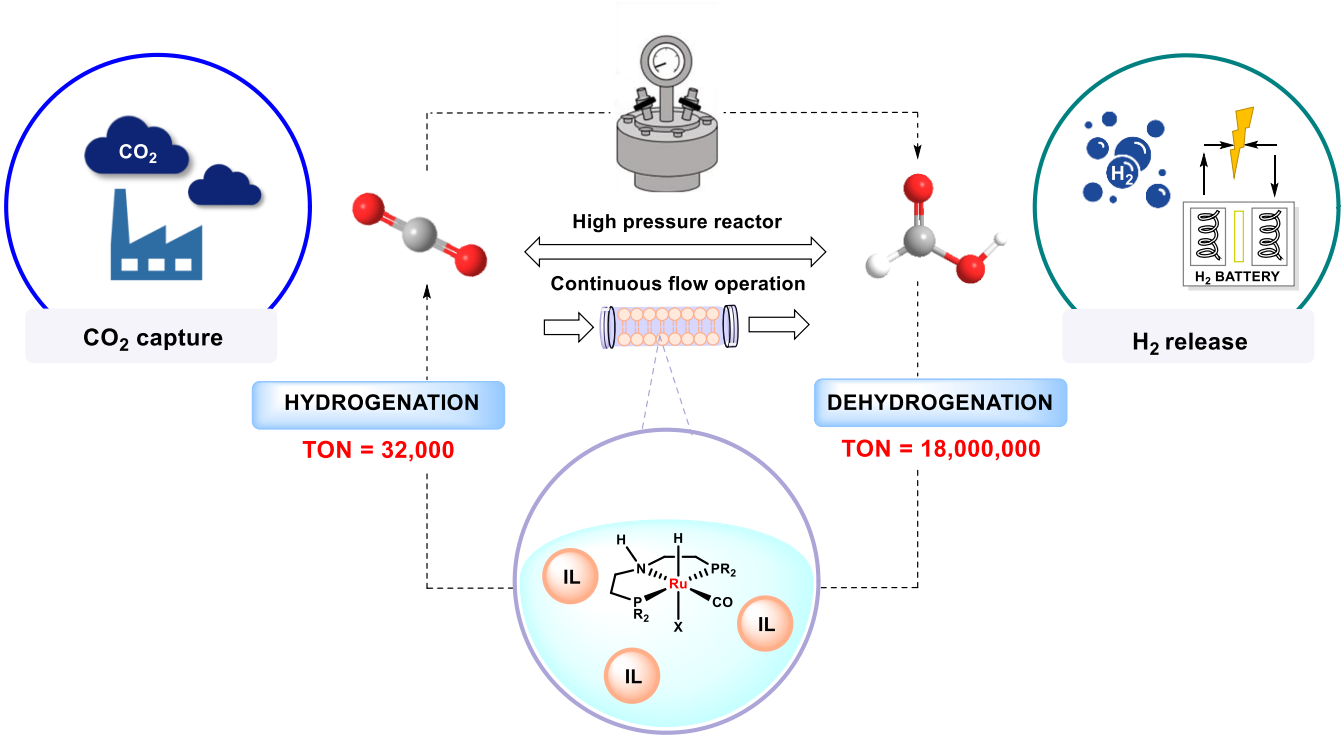
CO2
CO2 capture
High pressure reactor
Continuous flow operation
H2
H2 BATTERY
H2 release
HYDROGENATION
TON = 32,000
DEHYDROGENATION
TON = 18,000,000
IL
IL
IL
H
N
H
Ru
PR2
CO
P
R2
X